Electronic Supplementary Information

Synthesis of Multifunctional CuFe₂O₄-Reduced Graphene Oxide Nanocomposite: An Efficient Magnetically Separable Catalyst as well as High Performing Supercapacitor and First-Principles Calculations for its Electronic Structures

Madhurya Chandel, Debabrata Moitra, Priyanka Makkar, Harshit Sinha, Harshdeep Singh Hora, and Narendra Nath Ghosh*

Nano-materials Lab, Department of Chemistry, Birla Institute of Technology and Science, Pilani K K Birla Goa Campus, Goa- 403726, India.

Synthesis of Graphene oxide (GO)

Graphene oxide was synthesized using graphite powder as reported by Hummers and Offeman.[1] In this synthesis method, 1g of graphite powder and 0.6g of $NaNO_3$ were mixed with 35 ml of H_2SO_4 at 0 °C. The mixture was stirred for 6 h, and then 3.8 g of $KMnO_4$ was added. The temperature was maintained at 35 °C for 8 h for complete oxidation of graphene sheets. After that 60ml of deionized water was added slowly and kept the temperature at 98 °C for 1 h with constant stirring. Then 2 ml of 30% H_2O_2 was added and stirred for 0.5 h. The mixture was centrifuged and washed with 10% HCl and distilled water. The yellowish brown precipitate of graphene oxide was obtained and dried at 60 °C.

Computational details

In case of $CuFe_2O_4$ a Monkhorst-Pack mesh of k-points 8×8×8 is used, to sample the Brillouin zone for geometry optimization and for calculating the density of states. The initial superlattice structure of graphene was constructed using a 2×2×1 super cell with 8 atoms and 15 Å vacuum space at z-axis and optimized using 4×4×1 Monkhorst-Pack k point grid.[2-3]

The density of states was calculated using 8×8×1 k point grid. In case of $CuFe_2O_4$-graphene composite, the relaxed structure of $CuFe_2O_4$ with $Fd\bar{3}m$ space group and graphene were used for constructing the superlattice structure.[4]

The superlattice was constructed using a 2 layer slab of $CuFe_2O_4$ crystal cleaved along (111) plane with a graphene layer placed 2 Å above the slab. Here, 4×4×1 k point grids were used for optimization of structure and density of states calculations respectively.[2] The sizes of the unit cells of the systems simulated are listed in Table S1.

Table S1 The sizes of the unit cells of simulated systems

System	Structural parameters	
$CuFe_2O_4$ Unit cell	a= b = c = 8.369 Å	$\alpha = \beta = \gamma = 90°$
Graphene	a= b = 4.9 Å ; c = 31.1 Å	$\alpha = \beta = 90°, \gamma = 120°$
$CuFe_2O_4$-slab	a= b = 5.91 Å ; c = 31.1 Å	$\alpha = \beta = 90°, \gamma = 120°$
$CuFe_2O_4$ -graphene	a= b = 5.56 Å; c = 31.1 Å	$\alpha = \beta = 90°, \gamma = 120°$
Strain on interface	ε_{11}= 2.48% , ε_{12}= 2.33%	
	Mean Absolute Strain = 2.09%	

Details of the input files for geometric optimization of the $CuFe_2O_4$ unit cell, $CuFe_2O_4$ (111) Slab, graphene superlattice and $CuFe_2O_4$-graphene superlattice

$CuFe_2O_4$ unit cell

```
&CONTROL
            title = 'Bulk' ,
        calculation = 'relax' ,
      restart_mode = 'from_scratch' ,
       wf_collect = .true. ,
          outdir = '/home/madhuriya/Pure-CuF/Bulk/' ,
          wfcdir = '/home/madhuriya/Pure-CuF/Bulk/' ,
        pseudo_dir='/opt/apps/quantum_espresso/qe-
6.1/pseudo/pslibrary.1.0.0/pbe/PSEUDOPOTENTIALS/' ,
          prefix = 'pwscf' ,
         verbosity = 'low' ,
           nstep = 200 ,
 /
 &SYSTEM
          ibrav = 2,
        celldm(1) = 15.8169242979704d0,
           nat = 14,
           ntyp = 3,
         ecutwfc = 30 ,
         ecutrho = 120 ,
        input_dft = 'pbe' ,
       occupations = 'smearing' ,
         degauss = 0.005d0 ,
```

```
              smearing = 'methfessel-paxton' ,
                 nspin = 2 ,
   starting_magnetization(1) = 2.00000e-01,
   starting_magnetization(2) = 2.00000e-01,
   starting_magnetization(3) = 0.00000e+01,
              vdw_corr = 'grimme-d2' ,
 /
 &ELECTRONS
       scf_must_converge = .false. ,
             conv_thr = 1d-06 ,
           adaptive_thr = .false. ,
            mixing_mode = 'local-TF' ,
            mixing_beta = 0.07d0 ,
 /
 &IONS
         ion_dynamics = 'bfgs' ,
/
ATOMIC_SPECIES
  Cu   63.54600  Cu.pbe-dn-rrkjus_psl.1.0.0.UPF
  Fe   55.84500  Fe.pbe-spn-rrkjus_psl.1.0.0.UPF
  O    15.99940  O.pbe-nl-rrkjus_psl.1.0.0.UPF
ATOMIC_POSITIONS crystal
  Cu     0.625000000    0.125000000    0.625000000
  Cu     0.625000000    0.625000000    0.125000000
  Fe     0.009095743   -0.009095743   -0.009095743
  Fe     0.240904257    0.259095743    0.259095743
  Fe     0.625000000    0.625000000    0.625000000
  Fe     0.125000000    0.625000000    0.625000000
  O      0.352246663    0.392577372    0.392577372
  O      0.365498515    0.400494493    0.868508477
  O      0.365498515    0.868508477    0.400494493
  O      0.862598593    0.392577372    0.392577372
  O      0.884501485    0.849505507    0.381491523
  O      0.897753337    0.857422628    0.857422628
  O      0.884501485    0.381491523    0.849505507
  O      0.387401407    0.857422628    0.857422628
K_POINTS automatic
 8 8 8  0 0 0
```

$CuFe_2O_4$ (111) plane Slab

```
&CONTROL
            title = 'CuF' ,
         calculation = 'relax' ,
        restart_mode = 'restart' ,
            wf_collect = .true. ,
```

```
                outdir = '/home/madhuriya/Pure-CuF/CuF-Slab/' ,
                wfcdir = '/home/madhuriya/Pure-CuF/CuF-Slab/' ,
              pseudo_dir='/opt/apps/quantum_espresso/qe-
6.1/pseudo/pslibrary.1.0.0/pbe/PSEUDOPOTENTIALS/' ,
                prefix = 'pwscf' ,
              verbosity = 'high' ,
/
&SYSTEM
                ibrav = 0,
              celldm(1) = 11.1842544286d0,
                  nat = 28,
                  ntyp = 3,
                ecutwfc = 30 ,
                ecutrho = 240 ,
              input_dft = 'pbe' ,
            occupations = 'smearing' ,
                degauss = 0.005d0 ,
              smearing = 'marzari-vanderbilt' ,
                  nspin = 2 ,
    starting_magnetization(1) = 0.5,
              vdw_corr = 'grimme-d2' ,
/
&ELECTRONS
            electron_maxstep = 500,
            scf_must_converge = .false. ,
                conv_thr = 1d-08 ,
            mixing_mode = 'local-TF' ,
            mixing_beta = 0.05d0 ,
/
&IONS
          ion_dynamics = 'bfgs' ,
          ion_ position ='default'
/
CELL_PARAMETERS alat
    1.000000000   0.000000000   0.000000000
   -0.500000000   0.866025404   0.000000000
    0.000000000   0.000000000   2.984697837
ATOMIC_SPECIES
  Cu   63.54600  Cu.pbe-spn-rrkjus_psl.1.0.0.UPF
  Fe   55.84500  Fe.pbe-spn-rrkjus_psl.1.0.0.UPF
  O    15.99940  O.pbe-nl-rrkjus_psl.1.0.0.UPF
ATOMIC_POSITIONS crystal
  O     0.825488122   0.674511878   0.064183278
  O     0.342783272   0.157216728   0.071280193
  O     0.833083007   0.149084722   0.071946161
  O     0.350915278   0.666916993   0.071946161
```

```
Fe    0.173761693    0.326238307    0.105496714
Fe    0.500000000    0.000000000    0.136780442
Fe    0.826238307    0.673761693    0.168064170
 O    0.649084722    0.333083007    0.201614724
 O    0.166916993    0.850915278    0.201614724
 O    0.657216728    0.842783272    0.202280692
 O    0.174511878    0.325488122    0.209377607
Fe    0.333333333    0.166666667    0.273560885
Cu    0.833333333    0.166666667    0.273560885
Cu    0.333333333    0.666666667    0.273560885
 O    0.492154789    0.007845211    0.337744162
 O    0.009449939    0.490550061    0.344841077
 O    0.017581945    0.000250326    0.345507046
 O    0.499749674    0.482418055    0.345507046
Fe    0.840428360    0.659571640    0.379057599
Fe    0.166666667    0.333333333    0.410341327
Fe    0.492904973    0.007095027    0.441625055
 O    0.833583660    0.184248612    0.475175609
 O    0.315751388    0.666416340    0.475175609
 O    0.323883394    0.176116606    0.475841577
 O    0.841178544    0.658821456    0.482938492
Cu    0.000000000    0.000000000    0.547121770
Fe    0.000000000    0.500000000    0.547121770
Cu    0.500000000    0.500000000    0.547121770
K_POINTS automatic
 4 4 1  0 0 0
```

Graphene Superlattice

```
        title = 'GO' ,
     calculation = 'nscf' ,
    restart_mode = 'from_scratch' ,
     wf_collect = .true. ,
         outdir = '/home/madhuriya/Ag-Ni/GO/' ,
         wfcdir = '/home/madhuriya/Ag-Ni/' ,
        pseudo_dir='/opt/apps/quantum_espresso/qe-
6.1/pseudo/pslibrary.1.0.0/pbe/PSEUDOPOTENTIALS/' ,
         prefix = 'GO' ,
         verbosity = 'high' ,
 /
 &SYSTEM
          ibrav = 0,
        celldm(1) = 9.9333961239d0,
            nat = 8,
            ntyp = 1,
          ecutwfc = 50 ,
```

```
        ecutrho = 400 ,
          nbnd = 50,
        input_dft = 'pbe' ,
      occupations = 'smearing' ,
         degauss = 0.005d0 ,
        smearing = 'marzari-vanderbilt' ,
        vdw_corr = 'grimme-d2' ,
 /
 &ELECTRONS
          conv_thr = 1d-06 ,
        mixing_beta = 0.05d0 ,
 /
CELL_PARAMETERS alat
    1.000000000    0.000000000    0.000000000
   -0.500000000    0.866025404    0.000000000
    0.000000000    0.000000000    1.909176510
ATOMIC_SPECIES
   C   12.01070  C.pbe-n-rrkjus_psl.1.0.0.UPF
ATOMIC_POSITIONS crystal
   C    0.333700887    0.184686245    0.588347888
   C    0.833828241    0.184740171    0.588327913
   C    0.167059375    0.351339991    0.588321870
   C    0.667076192    0.351300916    0.588327069
   C    0.333654895    0.684633366    0.588332772
   C    0.833832636    0.684557864    0.588299815
   C    0.167079247    0.851343793    0.588302468
   C    0.667148522    0.851272881    0.588340545
K_POINTS automatic
 4 4 1   0 0 0
```

<u>$CuFe_2O_4$ (111)plane-graphene Superlattice</u>

```
 &CONTROL
          title = 'Interface' ,
        calculation = 'relax' ,
       restart_mode = 'from_scratch' ,
          outdir = '/home/madhuriya/Pure-CuF/Interface/' ,
          wfcdir = '/home/madhuriya/Pure-CuF/Interface/' ,
        pseudo_dir='/opt/apps/quantum_espresso/qe-
6.1/pseudo/pslibrary.1.0.0/pbe/PSEUDOPOTENTIALS/' ,
          prefix = 'pwscf' ,
        verbosity = 'high' ,
          nstep = 200 ,
 /
 &SYSTEM
```

```
           ibrav = 0,
        celldm(1) = 10.5217793346d0,
            nat = 36,
           ntyp = 4,
         ecutwfc = 30 ,
         ecutrho = 240 ,
       input_dft = 'pbe' ,
      occupations = 'smearing' ,
         degauss = 0.005d0 ,
        smearing = 'marzari-vanderbilt' ,
           nspin = 2 ,
  starting_magnetization(1) = 0.5,
         vdw_corr = 'grimme-d2' ,
 /
 &ELECTRONS
     scf_must_converge = .false. ,
          conv_thr = 1d-08 ,
       mixing_mode = 'local-TF' ,
       mixing_beta = 0.05d0 ,
 /
 &IONS
        ion_dynamics = 'bfgs' ,
        ion_positions = 'default' ,
      trust_radius_max = 1.2 ,
 /
CELL_PARAMETERS alat
   1.000000000    0.000000000    0.000000000
  -0.500000000    0.866025404    0.000000000
   0.000000000    0.000000000    4.975035579
ATOMIC_SPECIES
  C   12.01070  C.pbe-n-rrkjus_psl.1.0.0.UPF
  Cu  63.54600  Cu.pbe-spn-rrkjus_psl.1.0.0.UPF
  Fe  55.84500  Fe.pbe-spn-rrkjus_psl.1.0.0.UPF
  O   15.99940  O.pbe-nl-rrkjus_psl.1.0.0.UPF
ATOMIC_POSITIONS crystal
  O    0.331757865    0.168242135    0.049842352
  O    0.836685839    0.172572407    0.053486328
  O    0.327427593    0.663314161    0.053486328
  O    0.826645982    0.673354018    0.055526283
  Fe   0.168067552    0.331932448    0.065682134
  Fe   0.497324207    0.002675793    0.075252501
  Fe   0.825424891    0.674575109    0.112409449
  O    0.661273515    0.838726485    0.133984412
  O    0.638567825    0.341624625    0.134217816
  O    0.158375375    0.861432175    0.134217816
  O    0.172391552    0.327608448    0.138058878
```

```
Cu    0.832114721   0.169515375   0.172098881
Cu    0.330484625   0.667885279   0.172098881
Fe    0.325477944   0.174522056   0.172831230
O     0.491550179   0.008449821   0.208435883
O     0.019916546   0.480083454   0.219568024
O     0.036091855   0.020681369   0.220910040
O     0.479318631   0.463908145   0.220910040
Fe    0.840700887   0.659299113   0.240915090
Fe    0.170981163   0.329018837   0.261264608
Fe    0.489202082   0.010797918   0.275419305
O     0.836454992   0.156193889   0.300031281
O     0.343806111   0.663545008   0.300031281
O     0.322010332   0.177989668   0.304873837
O     0.848333984   0.651666016   0.312567769
Fe    0.024557333   0.475442667   0.330573325
Cu    0.506237702   0.507847952   0.344659584
Cu    0.992152048   0.993762298   0.344659584
C     0.833763805   0.684619934   0.453741408
C     0.167093236   0.851329636   0.453742499
C     0.167070265   0.351356009   0.453748185
C     0.667085054   0.351297097   0.453748368
C     0.833746390   0.184622583   0.453748939
C     0.333777030   0.684680425   0.453749320
C     0.667110629   0.851297223   0.453751175
C     0.333733586   0.184672319   0.453752573
K_POINTS automatic
 4 4 1   0 0 0
```
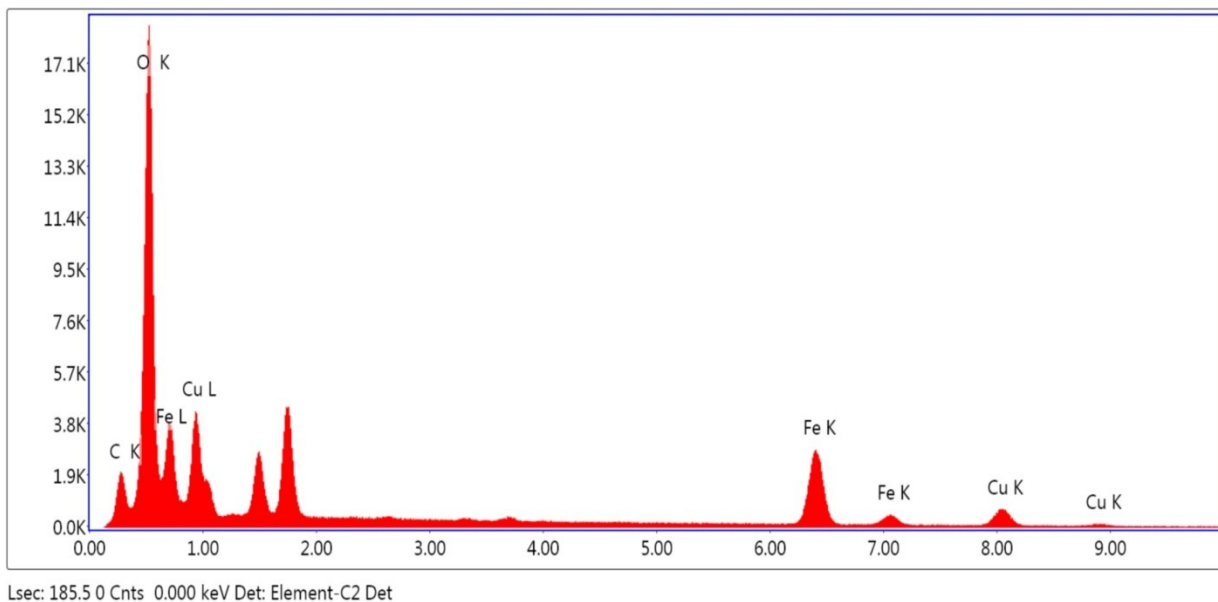
Fig. S1 EDS spectra of synthesized 96CuFe$_2$O$_4$-4RGO nanocomposite.
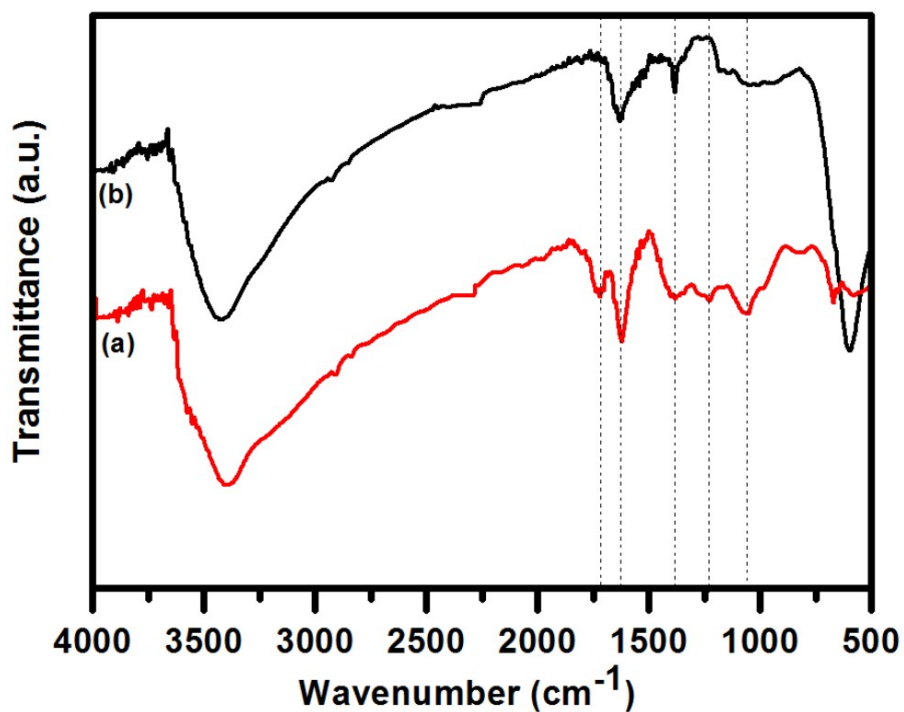
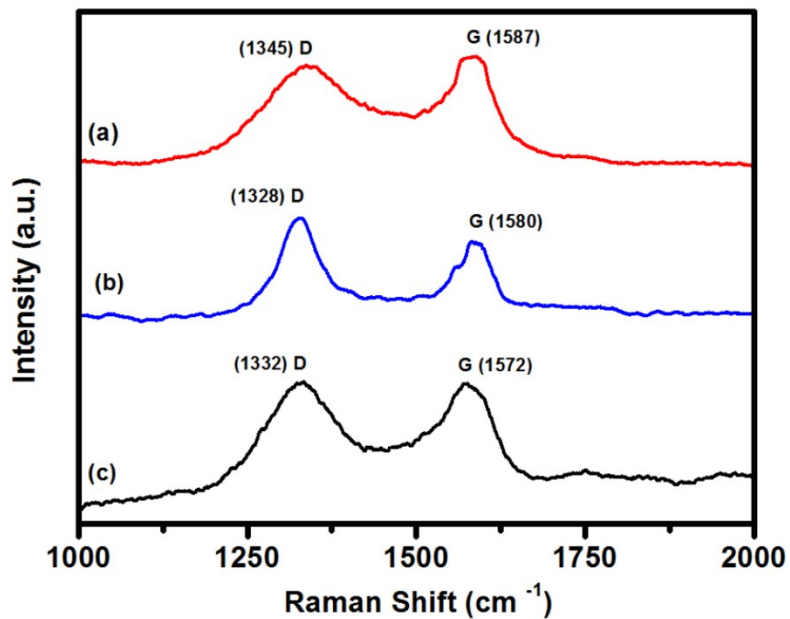**Fig. S2** FT-IR spectra of (a) GO, and (b) 96CuFe$_2$O$_4$-4RGO nanocomposite.

Fig. S3 Raman spectra of (a) GO, (b) RGO, and (c) 96CuFe$_2$O$_4$-4RGO nanocomposite.
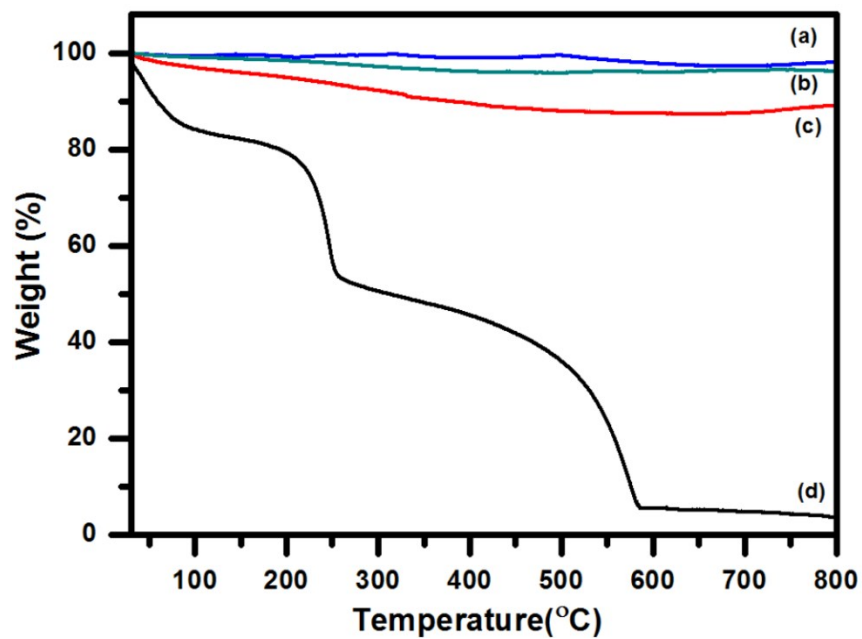
Fig. S4 TGA curve of (a) pure CuFe$_2$O$_4$, (b) 96CuFe$_2$O$_4$-4RGO, (c) 92CuFe$_2$O$_4$-8RGO nanocomposite, and (d) GO.
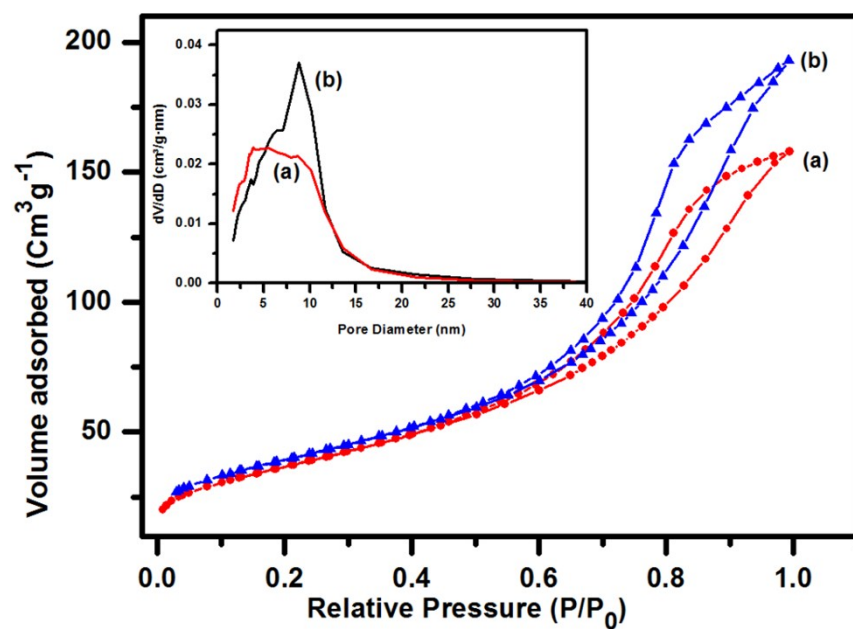
Fig. S5 N$_2$ adsorption-desorption isotherms and (inset) pore size distribution of synthesized (a) pure CuFe$_2$O$_4$ and (b) 96CuFe$_2$O$_4$-4RGO nanocomposite.
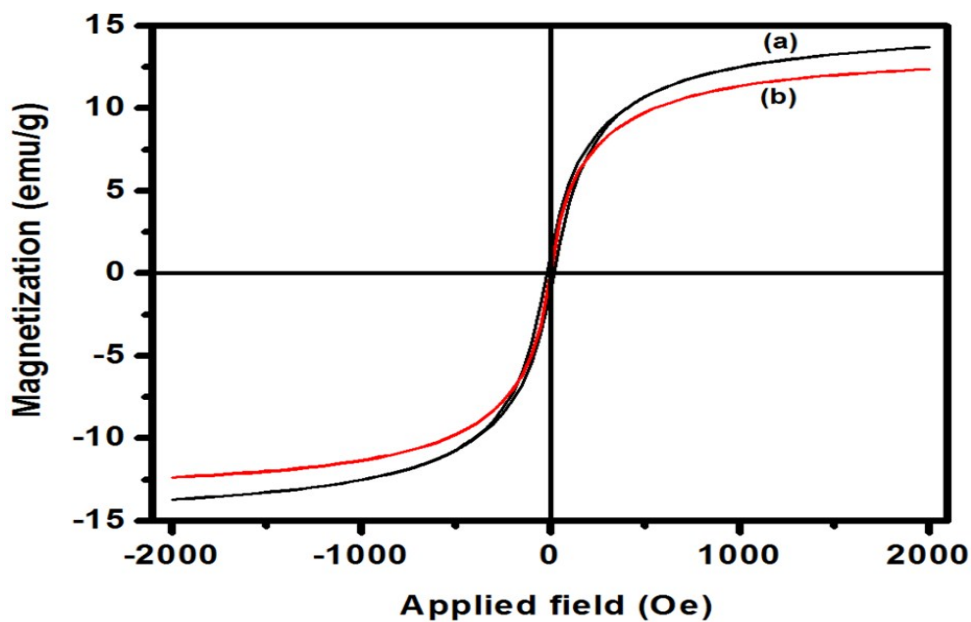
Fig. S6 Room temperature magnetic hysteresis loops of (a) pure CuFe$_2$O$_4$, (b) 96CuFe$_2$O$_4$-4RGO.
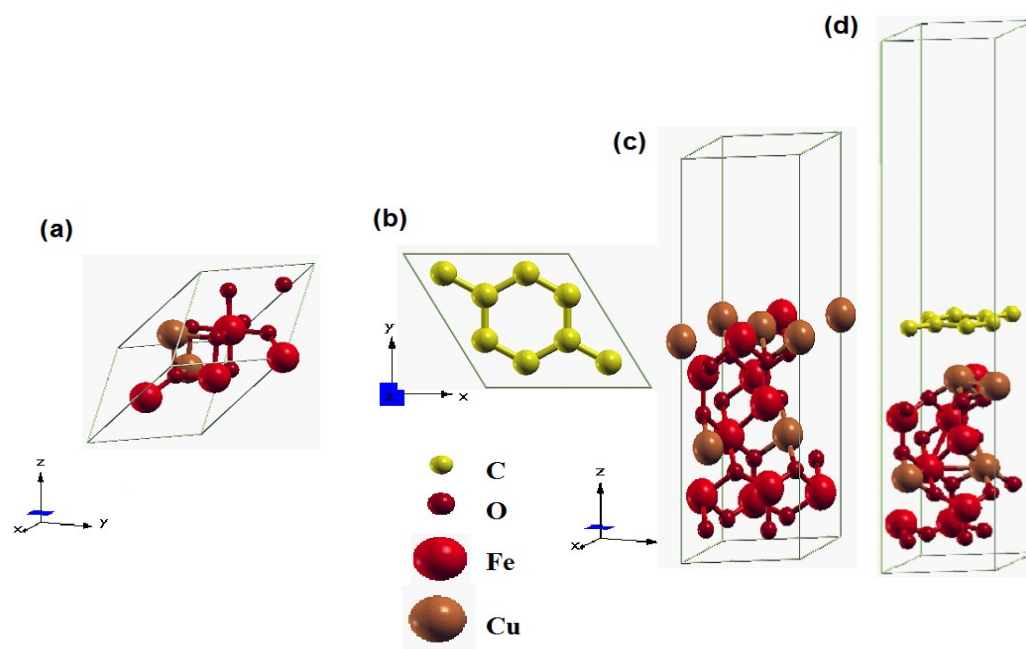
Fig. S7 The initial structure of (a) CuFe$_2$O$_4$ unit cell, (b) graphene superlattice, (c) CuFe$_2$O$_4$ (111) slab, and (d) CuFe$_2$O$_4$-graphene superlattice.
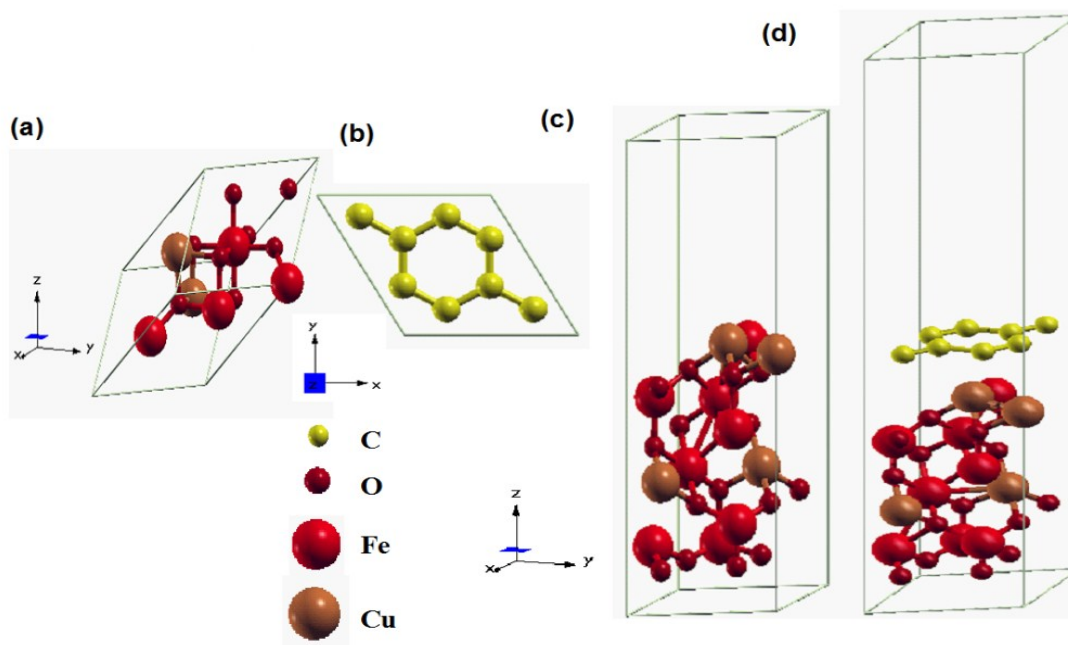
Fig. S8 The optimized structure of (a) CuFe$_2$O$_4$ unit cell, (b) graphene superlattice, (c) CuFe$_2$O$_4$ (111) slab and (d) CuFe$_2$O$_4$-graphene superlattice.

Table S2 Comparison of optimized structural parameter of graphene superlattice with the reported values.

Material	Structural Parameters	Positional Parameters	References
Graphene (P6/mmm space group)	a = 1.42 Å -	C(1): 0.1933, 0.1433, 0.8127; C(2): 0.6933, 0.1433, 0.8126; C(3): 0.3600, 0.3100, 0.8127; C(4): 0.8600, 0.3100, 0.8126; C(5): 0.1933, 0.6433, 0.8126; C(6): 0.6933, 0.6433, 0.8127; C(7): 0.3600, 0.8100, 0.8127; C(8): 0.8600, 0.8100, 0.8127;	[5]
	a = 1.42 Å	-	[6]
	a = 1.42 Å	**C(1): 0.1933, 0.1433, 0.8127;** **C(2): 0.6933, 0.1433, 0.8126;** **C(3): 0.3600, 0.3100, 0.8127;** **C(4): 0.8600, 0.3100, 0.8126;** **C(5): 0.1933, 0.6433, 0.8126;** **C(6): 0.6933, 0.6433, 0.8127;** **C(7): 0.3600, 0.8100, 0.8127;** **C(8): 0.8600, 0.8100, 0.8127;**	**This work**

Table S3 Comparison of the optimized structural parameter and band gap of $CuFe_2O_4$ unit cell with the reported values obtained by different theoretical calculations.

System	Method of optimization	Structural parameters	Band gap obtained from DFT calculation	References
$CuFe_2O_4$ ($Fd\bar{3}m$) Cubic	DFT	a= b = c =5.777 Å α = β = γ = 60 °	-	[4]
$CuFe_2O_4$ ($Fd\bar{3}m$) Cubic	DFT+U	a= b = c = 5.917 Å α = β = γ = 60 °	-	[4]
$CuFe_2O_4$	DFT	a= b = 5.976 Å, c = 5.676 Å α = β = 61.64 ° γ =57.03 °		[4]
$CuFe_2O_4$	DFT+U	a= b = 6.059 Å, c = 5.912 Å α = β = 60.80 ° γ =57.57º	1.429 eV (Indirect band gap)	[4]
$CuFe_2O_4$ ($Fd\bar{3}m$) Cubic	PBESOL and GGA+U	a= b = c = 8.389 Å α = β = γ = 90º	0.603 eV	[7]
$CuFe_2O_4$	GGA+U	a= b = 8.136 Å, c = 8.669 Å	1.2 eV	[8]
$CuFe_2O_4$ Cubic	GGA	a= b = c = 8.37 Å	-	[9]
$CuFe_2O_4$ ($Fd\bar{3}m$) Cubic	**PBE + Grimme-D2**	**a =b= c= 8.369 Å** **α = β = γ = 90º**	**1.62 eV (Majority) and 1.43 eV (Minority)**	**This work**

Table S4 Comparison of optimized structural parameter of $CuFe_2O_4$ unit cell with the reported experimental values.

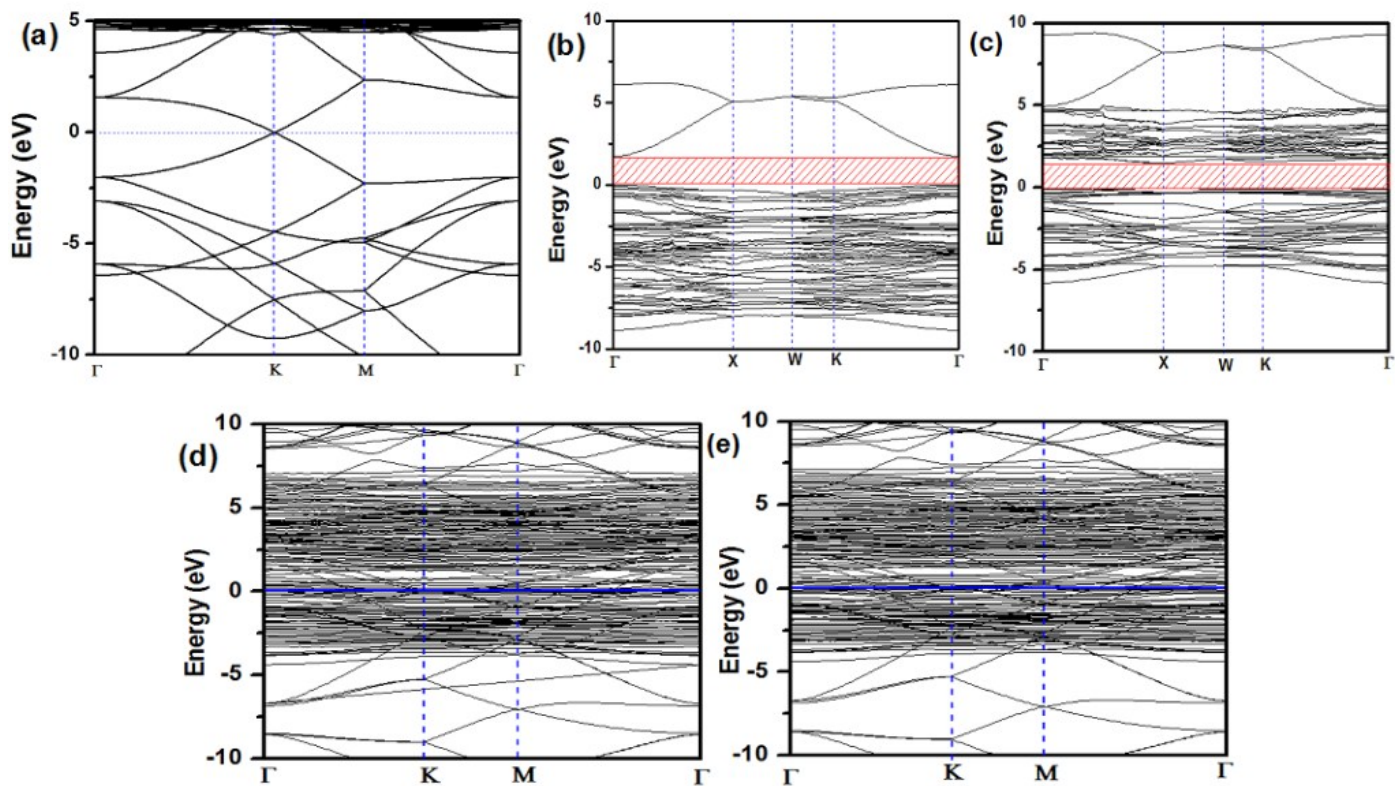| Material	Structural Parameters	References
$CuFe_2O_4$	a = 8.37 Å	[10]
Cubic	a = 8.371 Å	[11]
	a = 8.374 Å	[12]
	a = 8.390 Å	[13]
	a = 8.369 Å	**This work**

Fig. S9 Electronic band structures of (a) graphene superlattice, (b) $CuFe_2O_4$ unit cell for majority band, (c) $CuFe_2O_4$ unit cell for minority band, (d) $CuFe_2O_4$-graphene superlattice for spin-up, and (e) $CuFe_2O_4$-graphene superlattice for spin-down. The Fermi level is referenced to zero energy, as indicated by the dotted line.
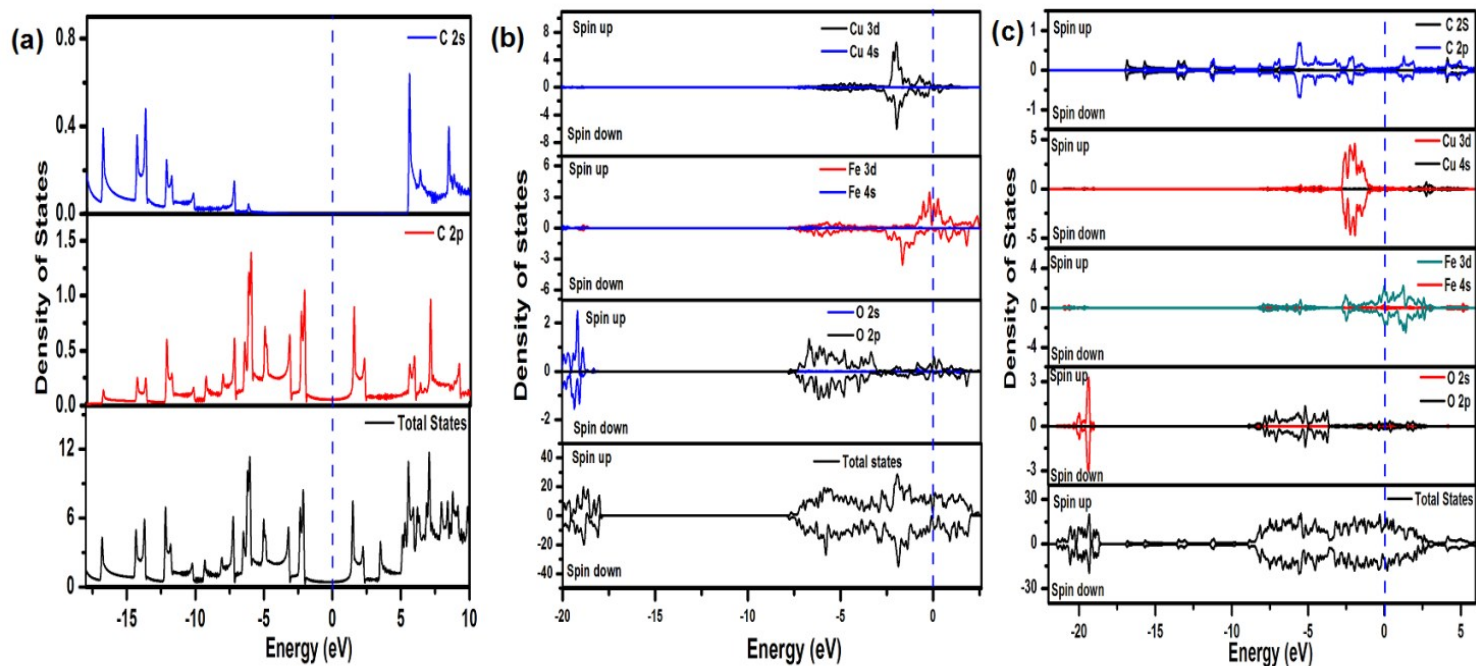
Fig. S10 Projected density of states of (a) graphene, (b) $CuFe_2O_4$ superlattice, and (c) $CuFe_2O_4$-graphene superlattice. The Fermi level is referenced to zero energy, as indicated by the dotted line.
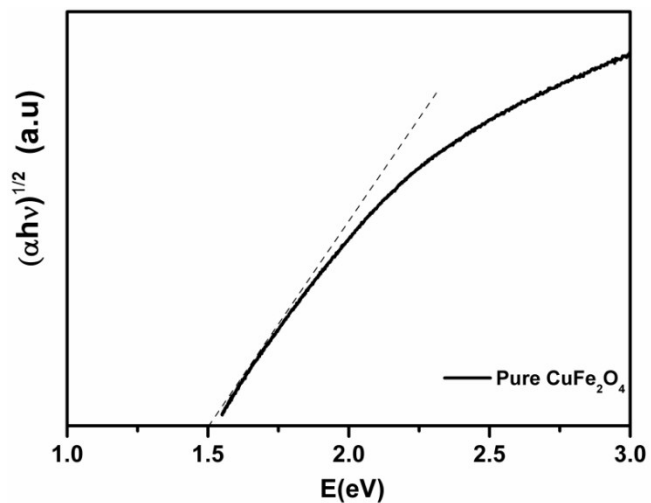

Fig. S11 The plot of transformed Kubelka-Munk function versus the energy of light for pure $CuFe_2O_4.$

Table S5 Reaction completion time and the apparent rate constant of reduction of 4-nitrophenol when the reaction was catalyzed by pure $CuFe_2O_4$ and different $CuFe_2O_4$-RGO nanocomposites.

Sr. no.	Composition of the catalyst	Reaction completion time (min)	Apparent rate constant (K_{app}) s^{-1}
1	Pure $CuFe_2O_4$	12	$5.7\ (\pm 0.3) \times 10^{-3}$
2	98 $CuFe_2O_4$-2RGO	7	$8.0\ (\pm 0.8) \times 10^{-3}$
3	96 $CuFe_2O_4$-4RGO	4	$17.2\ (\pm 0.6) \times 10^{-3}$
4	94 $CuFe_2O_4$-6RGO	5	$10.3\ (\pm 2.0) \times 10^{-3}$
5	92 $CuFe_2O_4$-8RGO	6	$9.8\ (\pm 1.0) \times 10^{-3}$

Table S6 Comparison of the catalytic efficiency of 96$CuFe_2O_4$-4RGO with various reported catalysts for the reduction reaction of 4-NP in presence of $NaBH_4$.

Catalyst	Rate Constant (K_{app})	Reference
Au nanoparticle	9.19×10^{-3} s^{-1}	[14]
Ag nanoparticle	4.06×10^{-3} s^{-1}	[14]
Cu nanoparticle	1.5×10^{-3} s^{-1}	[15]
Ag@SBA-15	1.7×10^{-3} s^{-1}	[16]
Au_1-Cu_3/rGO	96×10^{-3} s^{-1}	[17]

Ag@CoFe$_2$O$_4$	19.6×10^{-3} s^{-1}	[18]
Cu@SBA-15	17.3×10^{-3} s^{-1}	[19]
Ag@Fe$_3$O$_4$	5.8×10^{-3} s^{-1}	[20]
Fe$_3$O$_4$@SiO$_2$-Ag	7.6×10^{-3} s^{-1}	[21]
Au-Fe$_3$O$_4$	10.5×10^{-3} s^{-1}	[22]
Fe$_3$O$_4$/Cu	17.1×10^{-3} s^{-1}	[23]
Fe$_3$O$_4$@SiO$_2$-Au MNCs	14.2×10^{-3} s^{-1}	[24]
Iron Oxide@Ag Core-shell	14.5×10^{-3} s^{-1}	[25]
Ag@Fe$_3$O$_4$@C Core shell	17.1×10^{-3} s^{-1}	[26]
Cu@SBA-15@CoFe$_2$O$_4$	18.3×10^{-3} s^{-1}	[27]
10%Cu/SBA-15	8.3×10^{-3} s^{-1}	[28]
CoFe$_2$O$_4$/PPy/Pd	13.2×10^{-3} s^{-1}	[29]
Fe$_3$O$_4$/graphene/Pt	20.0×10^{-3} s^{-1}	[30]
Fe$_3$O$_4$/graphene/Pd	61.0×10^{-3} s^{-1}	[30]
Au/graphene hydrogel	3.17×10^{-3} s^{-1}	[31]
Ni-Ag@RGO	89×10^{-3} s^{-1}	[32]
Ni-RGO	1.8×10^{-3} s^{-1}	[33]
PtNi nanosnowflakes/RGO	2.17×10^{-3} s^{-1}	[34]
Ag-Au/rGO	3.47×10^{-3} s^{-1}	[35]
CuO$_{0.05}$ -rGO	231×10^{-3} s^{-1}	[36]
2.5Ru@SBA-15	13.5×10^{-3} s^{-1}	[37]

CuO@mTiO$_2$@CoFe$_2$O$_4$	12.0×10^{-3} s^{-1}	[38]
Ag@mTiO$_2$@CoFe$_2$O$_4$	18.0×10^{-3} s^{-1}	[39]
CuFe$_2$O$_4$	120.0×10^{-3} s^{-1}	[40]
50Ni$_{0.8}$Zn$_{0.2}$Fe$_2$O$_4$-50RGO	12.2×10^{-3} s^{-1}	[41]
98BiFeO$_3$-2RGO	12.0×10^{-3} s^{-1}	[42]
CuFe$_2$O$_4$	14.1 ×10^{-3} s^{-1}	[43]
NiFe$_2$O$_4$	1.9×10^{-3} s^{-1}	[43]
CuFe$_2$O$_4$	**4.2 ×10^{-3} s^{-1}**	**This work**
96CuFe$_2$O$_4$-4RGO	**17.2 ×10^{-3} s^{-1}**	**This work**
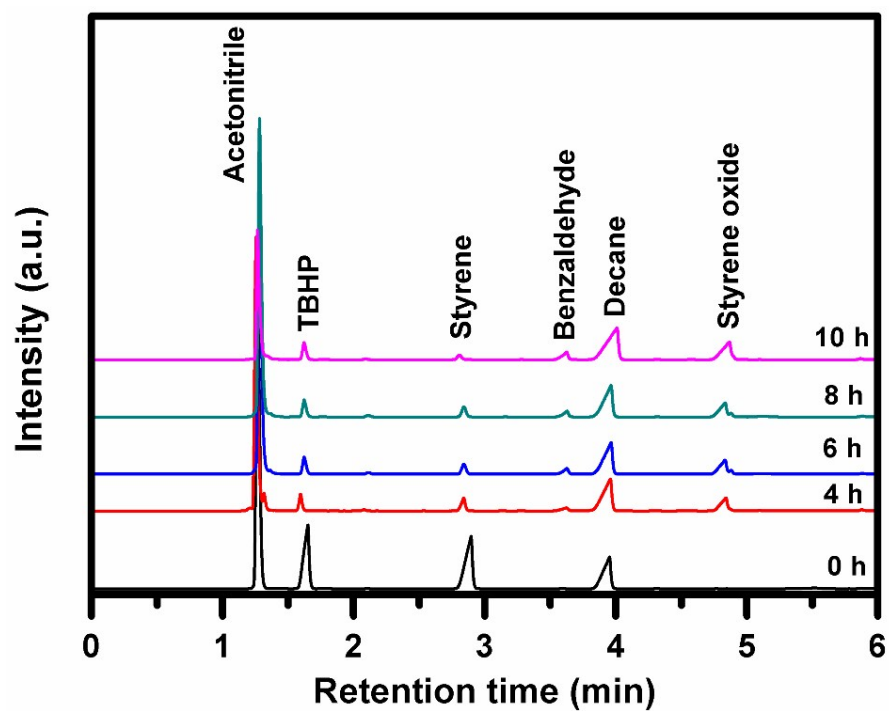
Fig. S12 Gas chromatography analysis of progress of $96CuFe_2O_4$-4RGO catalyzed styrene epoxidation reaction with time.

Table S7 Comparison of catalytic efficiency of different reported catalysts for the epoxidation reaction of styrene.

Catalyst	Styrene Conversion/ Yield (%)	Selectivity of Styrene Oxide formation (%)	Reference
Ag@m- TiO2@CoFe$_2$O$_4$	98	94	[39]
98BiFeO$_3$-2RGO	79	90	[42]
Ag-Fe$_3$O$_4$	100	84	[44]
Au(1wt.%)/BaTNT	60	80	[45]
CuO@mTiO2@CoFe$_2$O$_4$	98	77	[46]
Ag/4A Zeolite	80	89	[47]
TiO$_2$-Ag	83	66	[48]
CuO/nanotubes-450	94	46	[49]
CuO-1	100	44	[50]

Cu-S-SBA-15	84	15	[51]
Ag-Cu/Cu$_2$O CNFs	99	41	[52]
Fe$_3$O$_4$@SiO$_2$-NH$_2$-Cu	85	51	[53]
Au/L-Fe$_3$O$_4$	76	70	[54]
Fe$_3$O$_4$	43	74	[54]
Fe$_2$O$_3$	17	60	[55]
Ag-Ni$_{0.81}$Fe$_{2.19}$O$_4$	69	84	[56]
Ag-Zn$_{0.60}$Fe$_{2.40}$O$_4$	18	67	[56]
Mg$_{0.4}$Fe$_{2.6}$O$_4$	32	4	[57]
Sr$_{0.2}$Ca$_{0.8}$Fe$_2$O$_4$	49	95	[58]
Ce$_{0.3}$Co$_{0.7}$Fe$_2$O$_4$	90	-	[59]
Mg$_{0.5}$Cu$_{0.5}$Fe$_2$O$_4$	21	-	[60]
Ni$_{0.5}$Zn$_{0.5}$Fe$_2$O$_4$	30	-	[61]
NiFe$_2$O$_4$	31	-	[61]
ZnFe$_2$O$_4$	26	-	[61]
CaFe$_2$O$_4$	38	-	[62]
SrFe$_2$O$_4$	51	-	[63]
CuFe$_2$O$_4$	**85**	**37**	**This work**
96CuFe$_2$O$_4$-4RGO	**90**	**65**	**This work**
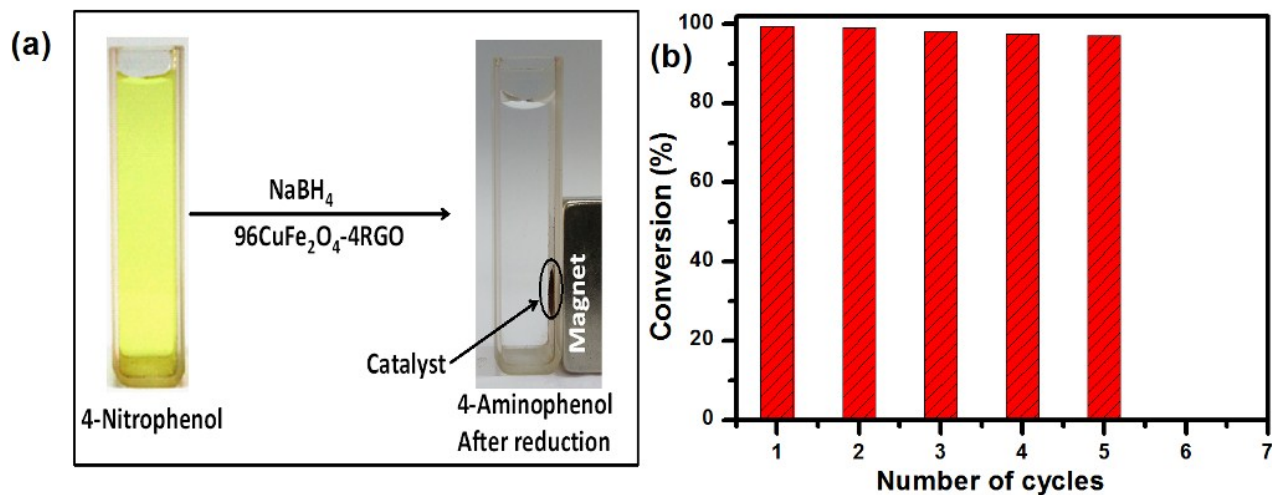
Fig. S13 (a) Magnetic separation of catalyst by applying a magnet externally after completion of the reaction and (b) Reusability of the catalyst for reduction of 4-NP.
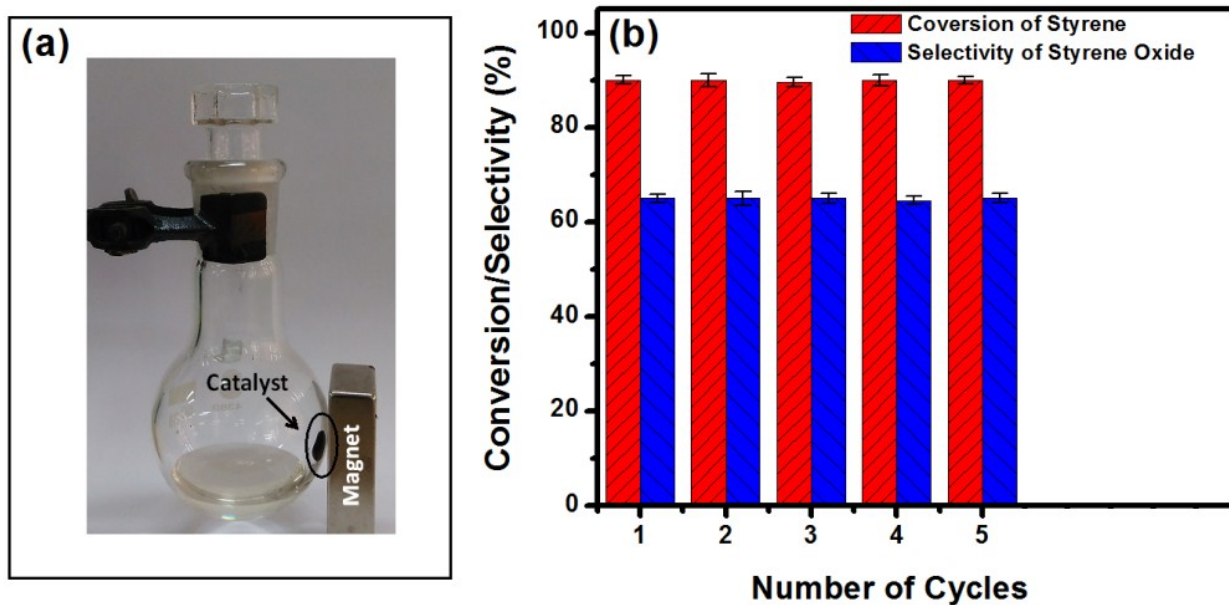

Fig. S14 (a) Magnetic separation of catalyst by applying a magnet externally after completion of the reaction and (b) Reusability of the catalyst for styrene epoxidation reaction.
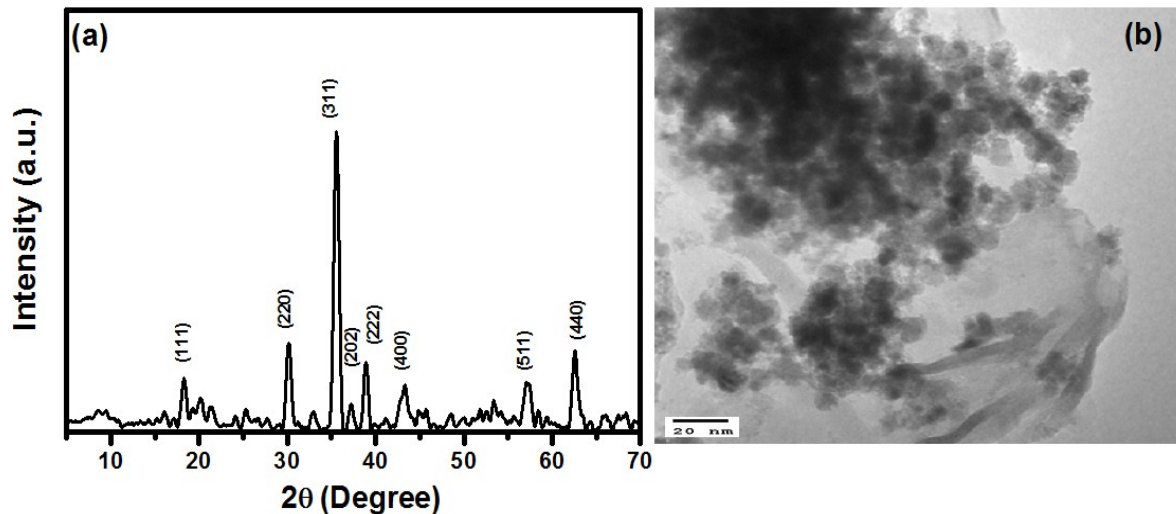
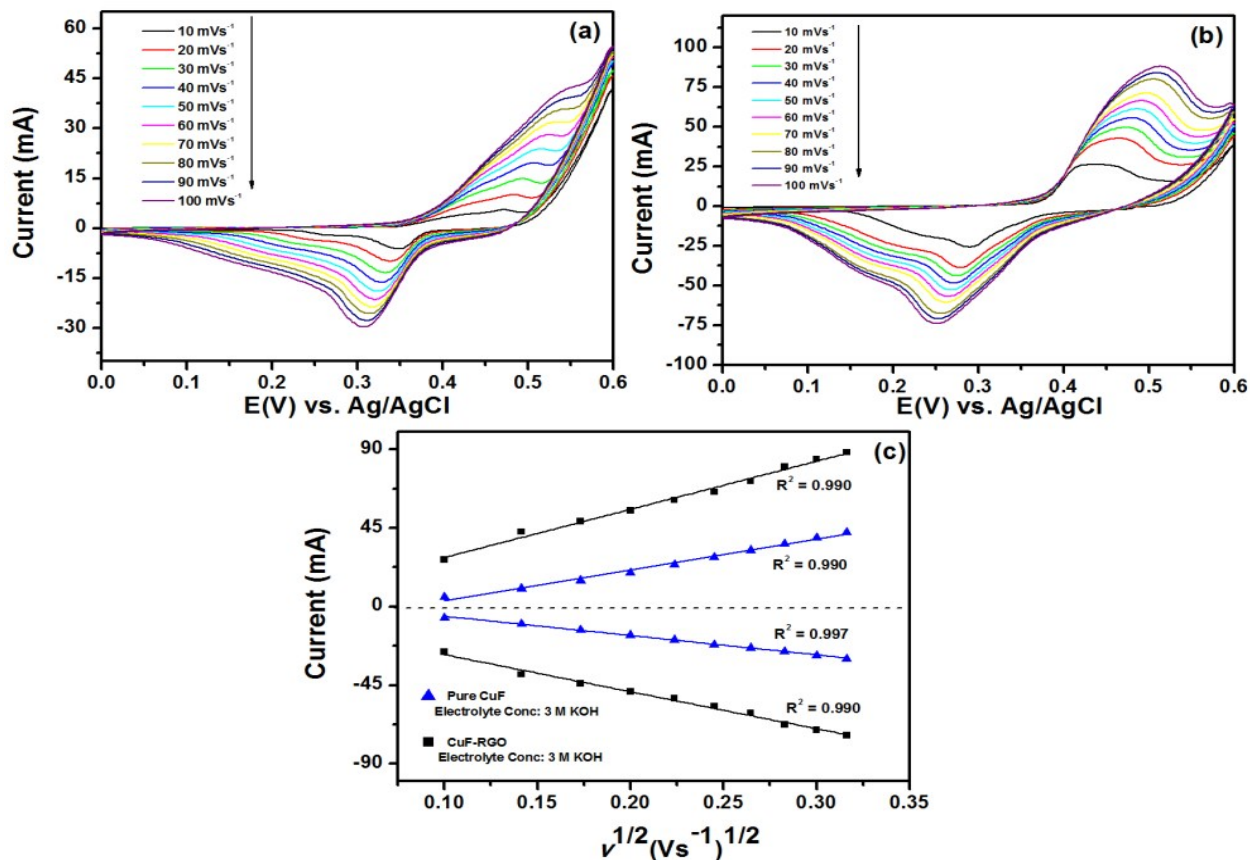**Fig. S15** (a) XRD and (b) TEM micrograph of the recycled 96CuFe$_2$O$_4$-4RGO catalyst.

Fig. S16 Cyclic voltammetry curves of (a) CuFe$_2$O$_4$ and (b) 96CuFe$_2$O$_4$-4RGO in 3 M KOH at different scanning rates (10−100 mV s^{-1}). (c) Randles-Sevcik plot for CuFe$_2$O$_4$ and 96CuFe$_2$O$_4$-4RGO nanocomposite in 3 M KOH.
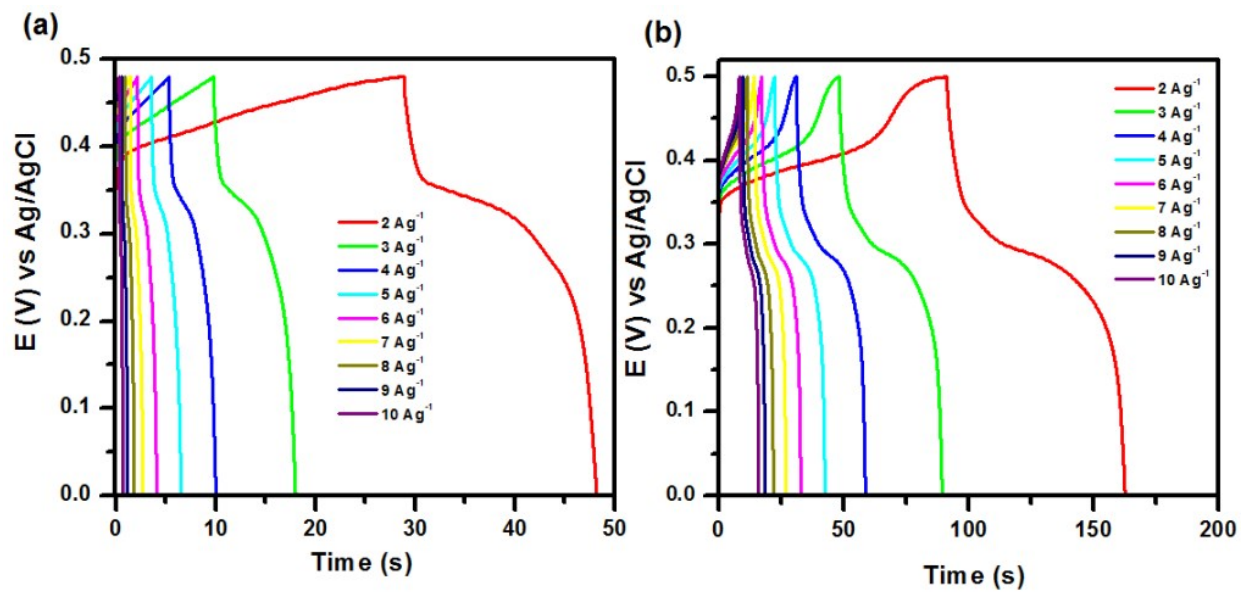
Fig.17 Galvanostatic charge-discharge curves of (a) pure $CuFe_2O_4$ and (b) $96CuFe_2O_4$-4RGO electrodes at different current densities (2 to10 A g^{-1}) in 3 M KOH.
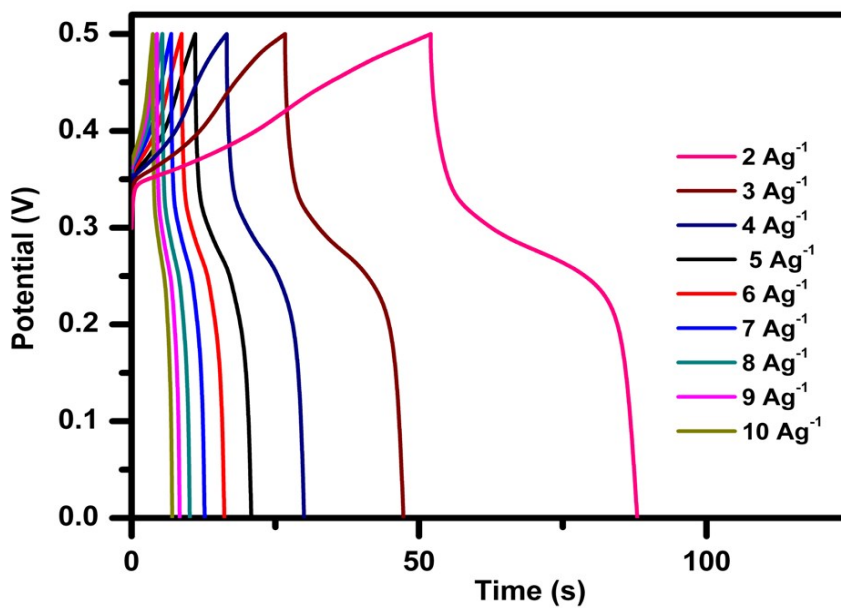

Fig. S18 Galvanostatic charge-discharge curves of RGO electrodes at different current densities (2 to 10 A g^{-1}) in 3 M KOH.
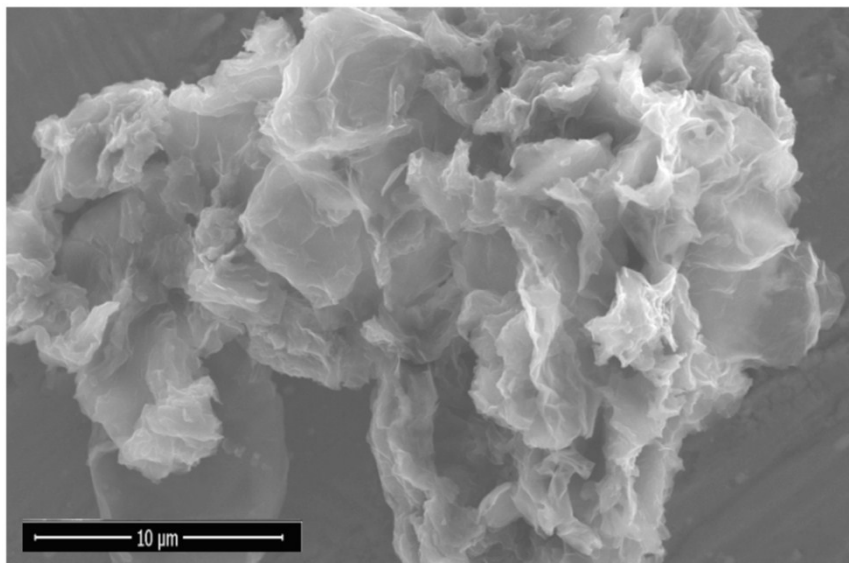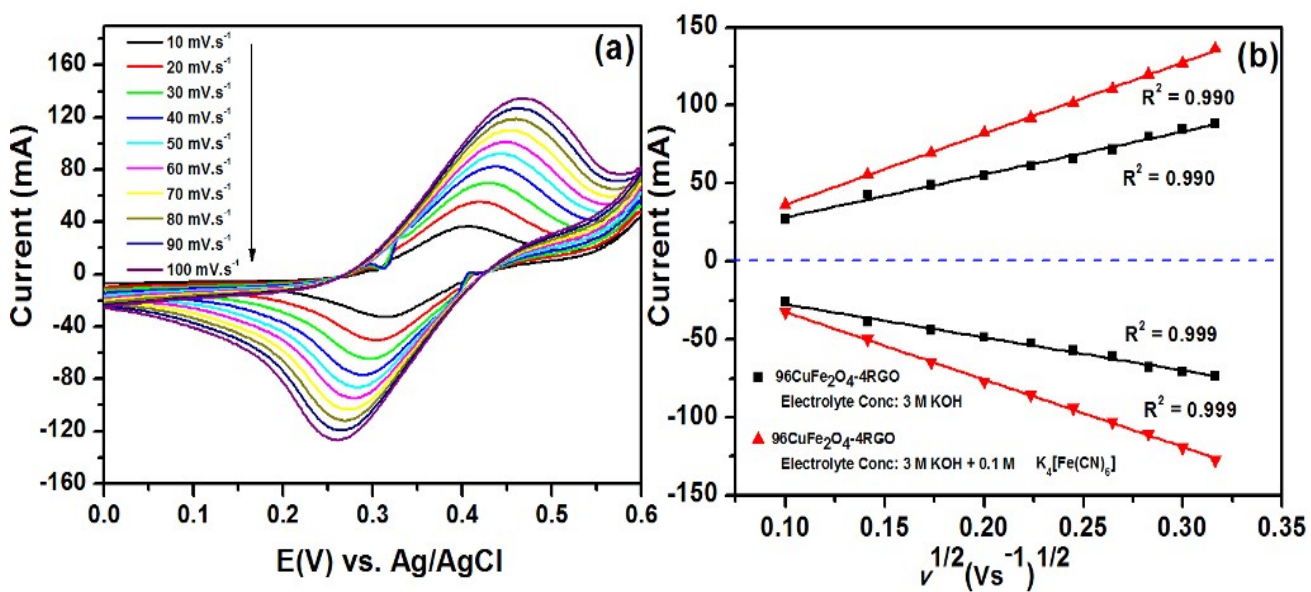
Fig. S19 FESEM micrograph of RGO.

Fig. S20 Cyclic voltammetry curves of (a) 96CuFe$_2$O$_4$-4RGO electrode in 3 M KOH + 0.1 M K$_4$[Fe(CN)$_6$]. at different scanning rates (10-100 mV s^{-1}). (b) Randles−Sevcik plots of the 96CuFe$_2$O$_4$-4RGO nanocomposite in 3 M KOH, and 3 M KOH + 0.1 M K$_4$[Fe(CN)$_6$].
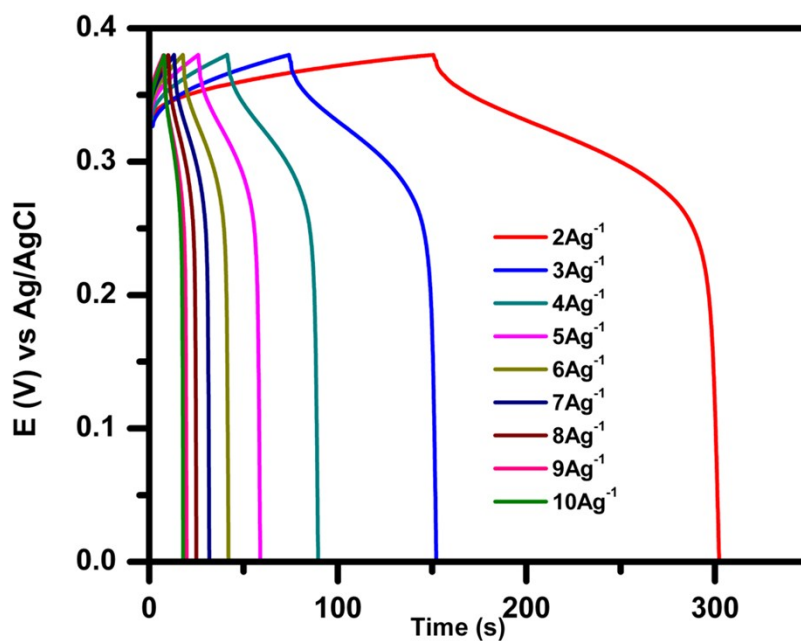
Fig. S21 Galvanostatic charge−discharge profile of $96CuFe_2O_4$-4RGO electrode in 3 M KOH + 0.1 M $K_4[Fe(CN)_6]$ with changing current density from 2 to 10 A g^{-1}.

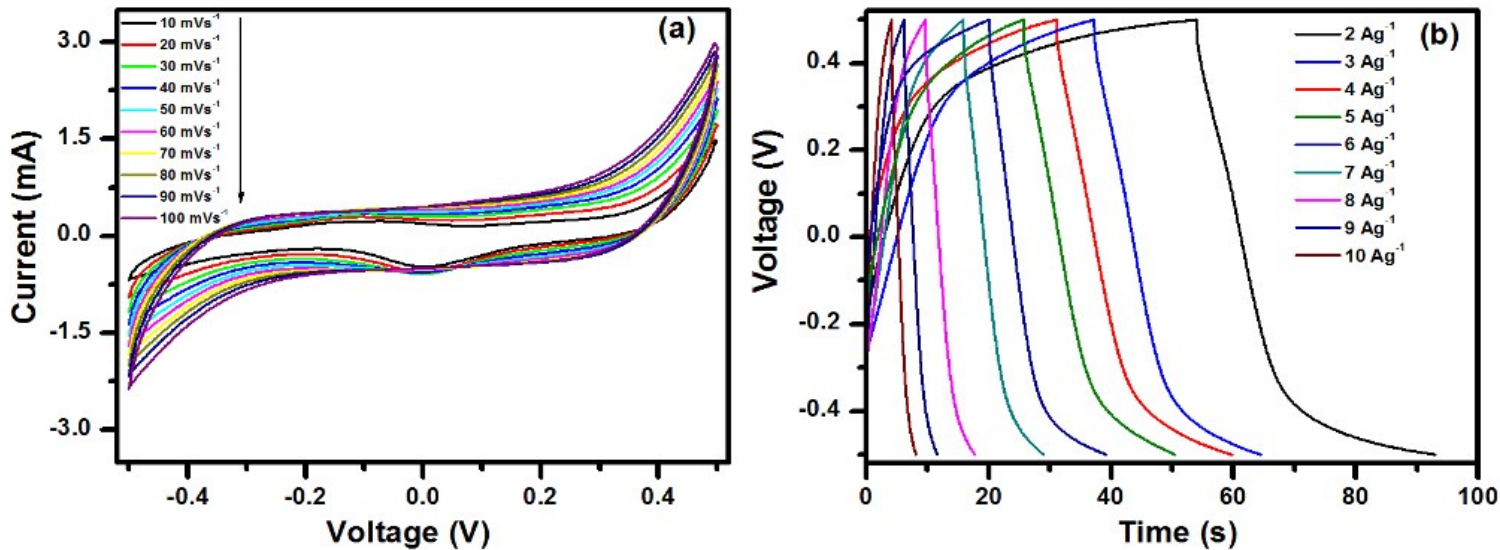**Fig. S22.** (a) Cyclic voltammetry curves at different scan rates (10-100 mV s^{-1}) and (b) galvanostatic charge−discharge curves with increasing current densities from 2 to 10 A g^{-1} of a $96CuFe_2O_4$-4RGO electrode in 3 M KOH + 0.1 M $K_4[Fe(CN)_6]$ in a two-electrode system.

Table S8 Comparison for different ferrite and ferrite-RGO based composite for supercapacitor application.

Material	Specific capacitance $(F\ g^{-1})$	Current Density $(A\ g^{-1})$	Electrolyte	Power Density $(W\ kg^{-1})$	Energy Density $(Wh\ kg^{-1})$	Reference
Graphene-NiFe$_2$O$_4$	345	1	1 M Na$_2$SO$_4$	-	-	[64]
ZnFe$_2$O$_4$/NRG	244	0.5	1 M KOH	3000	6.7	[65]
Fe$_3$O$_4$@carbon nanosheet	586	0.5	PVA-KOH	351	18.3	[66]
MnFe$_2$O$_4$/Graphene	120	0.1	(PVA)-H$_2$SO$_4$ gel	400	5.0	[67]
Cobalt Ferrite/Graphene/ Polyaniline	767.7	0.1	1 M KOH	178.2	79.7	[68]
Manganese ferrite/Graphene/ Polyaniline	307.2	0.1	1 M KOH	-	13.5	[69]
3D Fe$_3$O$_4$/rGO hybrids	455	3.6	2 M KOH	2740	80.9	[70]
Mg-Ferrite rose nano flower	240	20m Vs^{-1}	3 M KOH	-	-	[71]
ZnFe$_2$O$_4$-CNT	217 mAh g^{-1}	5 mV s^{-1}	1 M NaOH	377.86	12.80	[72]
MnCoFeO$_4$	675	1 mVs^{-1}	6 M KOH	337.50	18.85	[73]
Ni$_{0.8}$Zn$_{0.2}$Al$_{0.1}$Fe$_{1.9}$O$_4$/rGO	136.91	1	6 M KOH	-	16.80	[74]
MoO$_2$/ NiFe$_2$O$_4$	2105 mAh g^{-1}	4	3 M KOH	-	-	[75]

98BiFeO$_3$-2RGO	928.43	5	3 M KOH + 0.1 M K$_4$[Fe(CN)$_6$]	950	18.62	[76]
CuFe$_2$O$_4$	47		1 M KCl	1985.40	11.03	[77]
CuFe$_2$O$_4$ nanowires/CNT	267		1 M KCl	1880.1	62.67	[77]
CuFe$_2$O$_4$ nanosphere	334	0.6	1 M KOH	-	-	[78]
CuFe$_2$O$_4$ fiber	28	0.5	1 M KOH	-	-	[79]
CuFe$_2$O$_4$ film	5.7	0.3μAcm^{-2}	1 M NaOH	-	-	[80]
CuFe$_2$O$_4$	48.77	10 mV s^{-1}	1 M H$_2$SO$_4$	-	-	[81]
CuFe$_2$O$_4$-Fe$_2$O$_3$	638.24	10 mV s^{-1}	1 M H$_2$SO$_4$			[81]
CuFe$_2$O$_4$	81.5	1	3 M KOH	1130	1.4	[82]
CuFe$_2$O$_4$-GN	576.6	1	3 M KOH	1100	15.8	[82]
Pure CuFe$_2$O$_4$	**83**	**2**	**3 M KOH**	**460**	**2.4**	**This work**
96CuFe$_2$O$_4$-4RGO	**797**	**2**	**3 M KOH + 0.1 M K$_4$[Fe(CN)$_6$]**	**380**	**16**	**This work**

References

1. W. S. Hummers Jr and R. E. Offeman, *J. Am. Chem. Soc.*, 1958, **80**, 1339.
2. H. J. Monkhorst and J. D. Pack, *Phys. Rev. B*, 1976, **13**, 5188.
3. G. Giovannetti, P. Khomyakov, G. Brocks, V. v. Karpan, J. Van den Brink and P. J. Kelly, *Phys. Rev. Lett.*, 2008, **101**, 026803.
4. Z. Jiang, W. Zhang, W. Shangguan, X. Wu and Y. Teraoka, *J. Phys. Chem. C*, 2011, **115**, 13035.
5. D. Moitra, S. Dhole, B. K. Ghosh, M. Chandel, R. K. Jani, M. K. Patra, S. R. Vadera and N. N. Ghosh, J. Phys. Chem. C, 2017, **121**, 21290.
6. B. Luo, X. Wang, E. Tian, H. Gong, Q. Zhao, Z. Shen, Y. Xu, X. Xiao and L. Li, ACS Appl. Mater. Interfaces, 2016, **8**, 3340.
7. R. Zhang, Q. Yuan, R. Ma, X. Liu, C. Gao, M. Liu, C.-L. Jia and H. Wang, *RSC Adv*, 2017, **7**, 21926-21932.
8. X. Zuo, A. Yang, C. Vittoria and V. G. Harris, J. Appl. Phys, 2006, **99**, 08M909.
9. M. Feng, A. Yang, X. Zuo, C. Vittoria and V. G. Harris, *J. Appl. Phys,* 2010, **107**, 09A521.
10. J. Gomes, M. Sousa, F. Tourinho, J. Mestnik-Filho, R. Itri and J. Depeyrot, J. Magn. Magn. Mater., 2005, **289,** 184-187.
11. J. Gomes, M. Sousa, G. da Silva, F. Tourinho, J. Mestnik-Filho, R. Itri, G. d. M. Azevedo and J. Depeyrot, J. Magn. Magn. Mater., 2006, **300**, e213.
12. B. K. Chatterjee, K. Bhattacharjee, A. Dey, C. K. Ghosh and K. K. Chattopadhyay, Dalton Trans., 2014, **43**, 7930..
13. S. Schaefer, G. Hundley, F. Block, R. McCune and R. Mrazek, *Metallurgical Transactions*, 1970, **1,** 2557.
14. A. Gangula, R. Podila, L. Karanam, C. Janardhana and A. M. Rao, *Langmuir*, 2011, **27**, 15268.
15. P. Deka, R. C. Deka and P. Bharali, *New J. Chem.*, 2014, **38**, 1789.
16. B. Naik, S. Hazra, V. S. Prasad and N. N. Ghosh, *Catal. Commun.*, 2011, **12**, 1104..
17. L. Rout, A. Kumar, R. S. Dhaka, G. N. Reddy, S. Giri and P. Dash, *Appl. Catal., A*, 2017, **538**, 107.
18. B. Naik, S. Hazra, D. Desagani, B. K. Ghosh, M. K. Patra, S. R. Vadera and N. N. Ghosh, *RSC Adv.*, 2015, **5**, 40193.
19. B. K. Ghosh, S. Hazra, B. Naik and N. N. Ghosh, *Powder Technol.*, 2015, **269**, 371.
20. J.-R. Chiou, B.-H. Lai, K.-C. Hsu and D.-H. Chen, *J. Hazard. Mater.*, 2013, **248**, 394.
21. Y. Chi, Q. Yuan, Y. Li, J. Tu, L. Zhao, N. Li and X. Li, *J. Colloid Interface Sci.*, 2012, **383**, 96.
22. F.-h. Lin and R.-a. Doong, *J. Phys. Chem. C*, 2011, **115**, 6591.
23. Z. Z. Wang, S. R. Zhai, B. Zhai and Q. D. An, *Eur. J. Inorg. Chem.*, 2015, **10**, 1692.
24. J. Zheng, Y. Dong, W. Wang, Y. Ma, J. Hu, X. Chen and X. Chen, *Nanoscale*, 2013, **5**, 4894.
25. G. Sharma and P. Jeevanandam, *Eur. J. Inorg. Chem.*, 2013, **36**, 6126.
26. M. Zhu, C. Wang, D. Meng and G. Diao, *J. Mater. Chem.A* 2013, **1**, 2118.
27. B. K. Ghosh, S. Hazra and N. N. Ghosh, *Catal. Commun.*, 2016, **80**, 44.
28. J. Wang, X. Shao, G. Tian and W. Bao, *J. Porous Mater.*, 2018, *25*, 207.
29. W. Sun, X. Lu, Y. Xue, Y. Tong and C. Wang, *Macromol. Mater. Eng.*, 2014, **299**, 361.
30. X. Li, X. Wang, S. Song, D. Liu and H. Zhang, *Chemistry-A European Journal*, 2012, **18**, 7601.
31. J. Li, C.-y. Liu and Y. Liu, *J. Mater. Chem.*, 2012, **22**, 8426.
32. L. Zhang, T. Wu, X. Xu, F. Xia, H. Na, Y. Liu, H. Qiu, W. Wang and J. Gao, *J. Alloys Compd.*, 2015, **628**, 364.
33. Y. Tian, Y. Liu, F. Pang, F. Wang and X. Zhang, *Colloids Surf., A*, 2015, **464**, 96.
34. P. Song, J.-J. Feng, S.-X. Zhong, S.-S. Huang, J.-R. Chen and A.-J. Wang, *RSC Adv.*, 2015, **5**, 35551.
35. K. Hareesh, R. Joshi, D. Sunitha, V. Bhoraskar and S. Dhole, *Appl. Surf. Sci.*, 2016, **389**, 1050.
36. C. Sarkar and S. K. Dolui, *RSC Adv.*, 2015, **5**, 60763.
37. B. K. Ghosh, S. Hazra, B. Naik and N. N. Ghosh, *J. Nanosci. Nanotechnol.*, 2015, **15**, 6516.
38. B. K. Ghosh, D. Moitra, M. Chandel, M. K. Patra, S. R. Vadera and N. N. Ghosh, *Catal. Lett.*, 2017, **147**, 1061.
39. B. K. Ghosh, D. Moitra, M. Chandel, H. Lulla and N. N. Ghosh, *Mater. Res. Bull.*, 2017, **94**, 361.
40. J. Feng, L. Su, Y. Ma, C. Ren, Q. Guo and X. Chen, *Chem. Eng. J.*, 2013, **221**, 16.
41. D. Moitra, B. Ghosh, M. Chandel, R. Jani, M. Patra, S. Vadera and N. Ghosh, *RSC Adv.*, 2016, **6**, 14090.
42. D. Moitra, B. K. Ghosh, M. Chandel and N. N. Ghosh, *RSC Adv.*, 2016, **6**, 97941.
43. A. Goyal, S. Bansal and S. Singhal, *Int. J. Hydrogen Energy*, 2014, **39**, 4895.
44. D.-H. Zhang, G.-D. Li, J.-X. Li and J.-S. Chen, *Chem. Commun.*, 2008, **29**, 3414.
45. D. Nepak and D. Srinivas, *Appl. Catal., A*, 2016, **523**, 61.
46. B. K. Ghosh, D. Moitra, M. Chandel, M. K. Patra, S. R. Vadera and N. N. Ghosh, *Catal. Lett.*, 2017, **147**, 1061.
47. X. Hu, J. Bai, C. Li, H. Liang and W. Sun, *Eur. J. Inorg. Chem.*, 2015, **22**, 3758.
48. D. Yang, N. Yang and J. Ge, *CrystEngComm*, 2013, **15**, 7230.

49   C. Hu, L. Zhang, J. Zhang, L. Cheng, Z. Zhai, J. Chen and W. Hou, *Appl. Surf. Sci.*, 2014, **298**, 116.
50   G. Qiu, S. Dharmarathna, Y. Zhang, N. Opembe, H. Huang and S. L. Suib, *J. Phys. Chem. C*, 2011, **116**, 468.
51   Y. Yang, S. Hao, P. Qiu, F. Shang, W. Ding and Q. Kan, *Reac. Kinet., Mech. Cat.*, 2010, **100**, 363.
52   Q. Wang, C. Li, J. Bai, W. Sun and J. Wang, *J. Inorg. Organomet. Polym Mater.*, 2016, **26**, 488.
53   J. Sun, G. Yu, L. Liu, Z. Li, Q. Kan, Q. Huo and J. Guan, *Catal. Sci. Technol.*, 2014, **4**, 1246.
54   C. Huang, H. Zhang, Z. Sun, Y. Zhao, S. Chen, R. Tao and Z. Liu, *J Colloid Interface Sci.*, 2011, **364**, 298.
55   V. R. Choudhary, R. Jha and P. Jana, *Catal. Commun.*, 2008, **10**, 205.
56   D.-H. Zhang, H.-B. Li, G.-D. Li and J.-S. Chen, *Dalton Trans.*, 2009, **47**, 10527.
57   N. Ma, Y. Yue, W. Hua and Z. Gao, *Appl. Catal., A*, 2003, **251**, 39.
58   R. Y. Pawar, P. V. Adhyapak and S. K. Pardeshi, *Appl. Catal., A*, 2014, **478**, 129.
59   J. Tong, W. Li, L. Bo, H. Wang, Y. Hu, Z. Zhang and A. Mahboob, *J. Catal.*, 2016, **344**, 474.
60   X. Cai, H. Wang, Q. Zhang and J. Tong, *J. Sol-Gel Sci. Technol.*, 2014, **69**, 33.
61   D. Guin, B. Baruwati and S. V. Manorama, *J. Mol. Catal. A: Chem.*, 2005, **242**, 26.
62   S. K. Pardeshi and R. Y. Pawar, Mater. Res. Bull., 2010, **45**, 609.
63   S. K. Pardeshi and R. Y. Pawar, *J. Mol. Catal. A: Chem.*, 2011, **334**, 35.
64   Z. Wang, X. Zhang, Y. Li, Z. Liu and Z. Hao, *J. Mater. Chem. A*, 2013, **1**, 6393.
65   L. Li, H. Bi, S. Gai, F. He, P. Gao, Y. Dai, X. Zhang, D. Yang, M. Zhang and P. Yang, *Sci. Rep.*, 2017, **7**, 43116.
66   H. Fan, R. Niu, J. Duan, W. Liu and W. Shen, *ACS Appl. Mater. Interfaces*, 2016, **8**, 19475.
67   W. Cai, T. Lai, W. Dai and J. Ye, *J. Power Sources*, 2014, **255**, 170.
68   P. Xiong, H. Huang and X. Wang, *J. Power Sources*, 2014, **245**, 937.
69   P. Xiong, C. Hu, Y. Fan, W. Zhang, J. Zhu and X. Wang, *J. Power Sources*, 2014, **266**, 384.
70   R. Kumar, R. K. Singh, A. R. Vaz, R. Savu and S. A. Moshkalev, *ACS Appl. Mater. Interfaces*, 2017, **9**, 8880.
71   K. Malaie, M. Ganjali, T. Alizadeh and P. Norouzi, *J Mater Sci-Mater El.*, 2018, 1.
72   S. S. Raut, B. R. Sankapal, M. Hossain, A. Shahriar, S. Pradhan, R. R. Salunkhe and Y. Yamauchi, *Eur. J. Inorg. Chem.*, 2018, **2**, 137.
73   A. E. Elkholy, F. E.-T. Heakal and N. K. Allam, *RSC Adv.*, 2017, **7**, 51888.
74   F. Meng, M. Yang, L. Zhao, Y. Zhang, X. Shang, P. Jin and W. Zhang, *Ceram. Int.*, 2017, **43**, 15959.
75   Y. Zhao, M. Yuan, Y. Chen, J. Yan, L. Xu, Y. Huang, J. Lian, J. Bao, J. Qiu and L. Xu, *Electrochim. Acta*, 2018, **260**, 439.
76   D. Moitra, C. Anand, B. K. Ghosh, M. Chandel and N. N. Ghosh, *ACS Appl. Energy Mater.*, 2018, **1**, 464.
77   S. Giri, D. Ghosh, A. P. Kharitonov and C. K. Das, *Funct. Mater. Lett.*, 2012, **5**, 1250046.
78   M. Zhu, D. Meng, C. Wang and G. Diao, *ACS Appl. Mater. Interfaces*, 2013, **5**, 6030.
79   J. Zhao, Y. Cheng, X. Yan, D. Sun, F. Zhu and Q. Xue, *CrystEngComm*, 2012, **14**, 5879.
80   D. Ham, J. Chang, S. Pathan, W. Kim, R. Mane, B. Pawar, O.-S. Joo, H. Chung, M.-Y. Yoon and S.-H. Han, *Curr. Appl Phys.*, 2009, **9**, S98.
81   R. Khan, M. Habib, M. A. Gondal, A. Khalil, Z. U. Rehman, Z. Muhammad, Y. A. Haleem, C. Wang, C. Q. Wu and L. Song, *Mater. Res. Express*, 2017, **4**, 105501.
82   W. Zhang, B. Quan, C. Lee, S.-K. Park, X. Li, E. Choi, G. Diao and Y. Piao, *ACS Appl. Mater. Interfaces A*, 2015, **7**, 2404.